Materials Research, Vol. 3, No. 4, 131-138, 2000.

Liquid Phase Sintered SiC. Processing and Transformation Controlled Microstructure Tailoring

V.A. Izhevskyi*, L.A. Genova, A.H.A. Bressiani, J.C. Bressiani

Instituto de Pesquisas Energéticas e Nucleares (IPEN),
Cidade Universitária, 05508-900 São Paulo - SP, Brazil

Received: August 3, 2000; Revised: October 6, 2000

Microstructure development and phase formation processes during sintering of silicon carbide based materials with AlN-Y_2O_3, AlN-Yb_2O_3, and AlN-La_2O_3 sintering additives were investigated. Densification of the materials occurred by liquid-phase sintering mechanism. Proportion of α- and β-SiC powders in the initial mixtures was a variable parameter, while the molar ratio of AlN/RE_2O_3, and the total amount of additives (10 vol. %) were kept constant. Shrinkage behavior during sintering in interrelation with the starting composition of the material and the sintering atmosphere was investigated by high temperature dilatometry. Kinetics of β-SiC to α-SiC phase transformation during post-sintering heat treatment at temperatures 1900-1950 °C was studied, the degree of phase transformation being determined by quantitative x-ray analysis using internal standard technique. Evolution of microstructure resulting from β-SiC to α-SiC transformation was followed up by scanning electron microscopy on polished and chemically etched samples. Transformation-controlled grain growth mechanism similar to the one observed for silicon nitride based ceramics was established. Possibility of in-situ platelet reinforced dense SiC-based ceramics fabrication with improved mechanical properties by means of sintering was shown.

Keywords: *silicon carbide, ceramics, sintering, phase formation, microstructure, phase transformation,* in-situ *reinforcement*

1. Introduction

Silicon carbide is considered to be an important structural ceramic material because of a promising combination of properties, such as high oxidation resistance, good mechanical properties retained to high temperatures, high wear resistance, good thermal shock resistance due to high thermal conductivity, etc. All these properties are inherent to silicon carbide due to highly covalent bonding. The latter, however, causes complications with sintering of SiC-based ceramics to high densities, which disadvantage is characteristic for all non-oxide covalent compounds, such as Si_3N_4 and AlN.

Unlike the aforementioned compounds, which tend to decompose severely at high temperatures, silicon carbide can be densified by solid-state sintering process at high temperatures of about 2100 °C with the aid of B and C[1], which dramatically improve the shrinkage kinetics. However, thus sintered materials have poor or, at the best, moderate mechanical properties (flexural strength of 300-450 MPA and fracture toughness of 2.5-4 $MPam^{-1/2}$). Liquid-phase sintering of SiC can be achieved at much lower temperatures (1800-1900 °C)[2,3] with the aid of metal oxides, such as Al_2O_3, Y_2O_3, and other rare-earth oxides[4-8]. The densification of SiC by liquid-phase sintering lately draws more attention because the materials processed by this method exhibit superior mechanical properties. The liquid phase sintering of SiC is somewhat similar to the same process for Si_3N_4. The oxide sintering aids react with SiO_2, which is always present at the surface of SiC particles, forming a silicate melt and enhancing densification. However, oxides interact with SiC with massive gasseous products formation leading to high weight loss and porosity[9,10]. It is known that alumina may interact with silicon carbide according to the following reactions[4]:

$$SiC\ (s) + Al_2O_3(s) \rightarrow Al_2O(g) + SiO(g) + CO(g)$$

$$2SiC(s) + Al_2O_3(s) \rightarrow Al_2O(g) + 2Si(l) + 2CO(g)$$

$$3SiC(s) + Al_2O_3(s) \rightarrow 2Al(l) + 3Si(l) + 3CO(g)$$

*invited scientist, on leave from the Institute for Problems of Materials Science, National Academy of Sciences of Ukraine, Kiev, Ukraine.
e-mail: izhevsky@net.ipen.br; jbressia@net.ipen.br

These reactions occur more actively with the increase of alumina content and the temperature of sintering. These reactions can be to some extent suppressed by the application of the high external partial pressure of CO and/or application of reactive powder beds[4]. However, such an approach is not completely effective and enables to achieve the final density not higher than 98% of theoretical density. Moreover, such techniques are costly and do not guarantee the reproducibility of materials properties.

Additional weight loss during liquid phase sintering of SiC occurs due to the reaction between SiC and SiO_2 surface films:

$$2SiO_2(s) + SiC(s) \rightarrow 3SiO(g) + CO(g)$$

It is therefore obvious that an alternative combination of sintering additives, which will eliminate or reduce the above-mentioned effects determined for densification, will be the best possible solution. As it was suggested by Chia *et al*[11], aluminum nitride, AlN, in combination with yttria, Y_2O_3, may present a solution. However, this possibility was not investigated in detail and only a limited amount of information is available[11,12]. Which is of additional interest, due to certain structural similarities SiC and AlN produce solid solutions and formation of mixed crystalline structures was observed[13-17].

By analogy with silicon nitride, it seems to be possible to tailor the microstructure and the structure-sensitive properties of silicon carbide based ceramics by varying α- to β-SiC ratio in the initial mixtures. If α-SiC is used as a starting powder, the final material is characterized by fine homogeneous microstructure with equiaxial grains[5,18], which results in moderate fracture toughness. Additions of β-SiC in combination with some specially developed thermal treatment leads to in-situ platelet reinforced material formation with improved mechanical properties[5,7,19].

In the present work sintering behavior and microstructure development of αβ-SiC-AlN-Y_2O_3/Yb_2O_3/La_2O_3 materials under conditions of pressureless sintering were investigated.

2. Experimental

Mixtures were prepared from high-purity powders of α-SiC (UF-15, H.C. Starck, Goslar, Germany), β-SiC (B10, H.C. Stark, Goslar, Germany), AlN (H.C. Starck, Germany, grade C), Y_2O_3 (99.98% purity, Aldrich Chemical Company, USA), Yb_2O_3 (99.9% purity, Aldrich Chemical Company, USA), and La_2O_3 (99.9% purity, Sigma-Aldrich Co., Switzerland) by attrition milling with alumina milling media in isopropyl alcohol for 4 h at 500 rpm. The total amount of sintering aids was kept constant at 10 vol.%. The ratio of α-SiC/β-SiC was a variable parameter, the content of α-SiC chosen as 5wt% and 10 wt.% relative to the amount of β-SiC. The ratio AlN/Y_2O_3 was kept constant at 3:2, the proportion chosen from the AlN–Y_2O_3 phase diagram[20] (see Fig. 1). The same molar ratio was chosen for both other RE sintering additives because of the known similarities between all RE oxides in regard of properties, and due to the absence of the data on phase relations between AlN and RE oxides with exception of aforementioned AlN-Y_2O_3 phase diagram.

The slurry obtained after attrition milling was separated from the milling media by passing through a ASTM 325 sieve and subsequently dried in a rotaevaporator. Samples of the mixture were taken for granulometric analysis and specific surface determination. The former was performed by means of laser granulometry (Granulometer 1064, CILAS, France), while the latter was accomplished by BET (ASAP 2000, Micrometrics Instrument Corp., USA). The process of drying was then completed in a drying box (48 h, 65 °C). Finally, the powder was passed through a ASTM 100 sieve to crush soft conglomerates.

Green bodies in the form of cylindrical pellets 20 mm in diameter and 25 mm height were prepared by consequent uniaxial pressing at 50 MPa, and cold isostatic pressing at 200 MPa. Dilatometric experiments were accomplished in a high temperature dilatometer (DIL 402 E/7, Netzsch GmbH, Germany) with a graphite resistance furnace and working parts in a flowing nitrogen or argon atmosphere. Sintering was accomplished in a gas-pressure furnace (Thermal Technologies, Santa Barbara, USA) with a graphite heating element in argon or nitrogen atmosphere under 1.5 MPa pressure. The flowchart of the materials processing is presented in Fig. 2.

Sintered samples were characterized for weight loss, density, phase composition and microstructure. Density was determined by Archimedes method. Phase composition was studied by X-ray diffraction (XRD) on a Siemens D-6000 powder diffractometer (Ni-filtered CuKα radia-

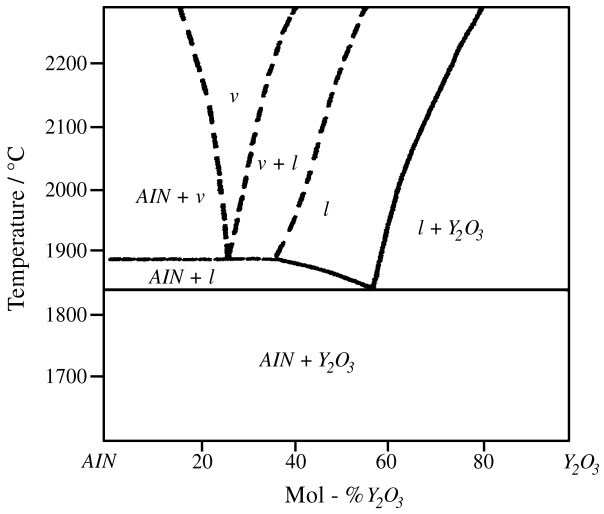

Figure 1. Behavioral diagram of the AlN-Y_2O_3 system.

tion, range of detection 10-80° 2Θ). Microstructure was studied by scanning electron microscopy (SEM) on a Phillips XL-30 and JEOL-JXA-6400 scanning electron microscopes with EDS analyzing attachment. Samples for microstructure investigation were prepared by standard ceramographic procedure of multistep grinding and polishing with subsequent chemical etching with Murakami's reagent (10 g of NaOH and 10 g of $K_3Fe(CN)_6$ in 40 mL H_2O at 110 °C for 20 to 30 min) for structural elements revelation.

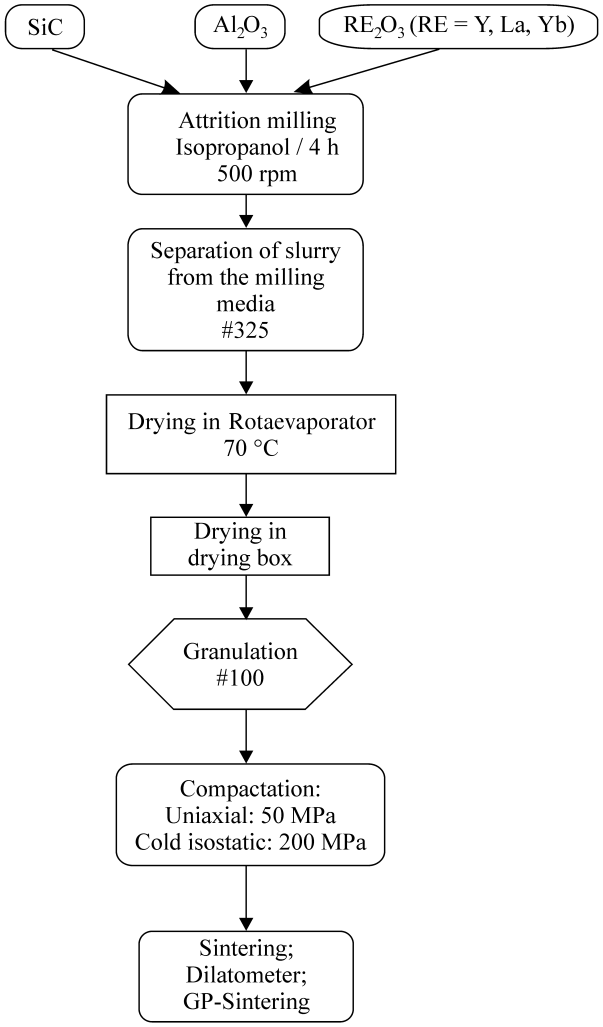

Figure 2. The flowchart of the materials processing.

3. Results and Discussion

The nominal formulation of the prepared mixtures together with some of their granulometric characteristics are presented in Table 1.

As it can be noted, the prepared mixtures can be described as having a narrow particle size distribution, and are of submicron fineness, which suggests favorable sintering behavior.

The results of the dilatometric investigations of the densification behavior of the prepared compositions under different sintering atmosphere – flowing nitrogen and flowing argon - are presented in Figs. 3 to 6. In Figs. 3 and 5, the linear shrinkage is plotted *vs.* temperature in nitrogen and in argon sintering atmosphere, respectively, and in Figs. 4 and 6 the shrinkage rate is plotted *vs.* temperature for the two sintering atmospheres used. As it can be seen, the behavior of the compositions under investigation is strikingly different depending on the sintering atmosphere.

As it can be observed from the linear shrinkage *vs.* temperature curves obtained while sintering in argon, the behavior of Y_2O_3 and Yb_2O_3 containing compositions is quite similar, while the La_2O_3 containing compositions show very poor densification (Figs. 5 (a) and (b)). The same can be stated for the shrinkage rate observed in argon atmosphere (Figs. 6 (a) and (b)), where the lowest shrinkage rate was observed for the La_2O_3 containing compositions as well. Additionally, for the latter compositions the beginning of shrinkage is shifted towards higher temperatures in relation to both other groups of compositions for about 200 °C. The maximum of shrinkage rate corresponds to about 1730, 1780, and 1850 °C for Y_2O_3, Yb_2O_3, and La_2O_3 containing compositions, respectively. The increase of α-SiC content from 5 to 10 wt.% in the initial mixture in this

Table 1. Characteristics of the starting powder and powders mixtures.

Material	α-SiC wt. %	β-SiC wt. %	Y_2O_3 wt. %	La_2O_3 wt. %	Yb_2O_3 wt. %	AlN wt. %	Grain size distribution			Specific surface area
							d_{10} [μm]	d_{50} [μm]	d_{90} [μm]	m^2/g
SiC5	4.32	82.13	10.65	-	-	2.90	<0.1	0.38	0.99	13.4
SiC10	8.65	77.80	10.65	-	-	2.90	<0.1	0.40	1.05	12.9
SiL5	4.13	78.42	-	14.68	-	2.77	<0.1	0.39	1.00	13.2
SiL10	8.26	74.29	-	14.68	-	2.77	<0.1	0.38	1.01	13.1
SiY5	3.86	73.34	-	-	19.79	3.09	<0.1	0.39	1.03	13.2
SiY10	7.71	69.41	-	-	19.79	3.09	<0.1	0.40	1.02	13.1

case has only a minor effect on densification behavior slightly hindering densification for all compositions investigated.

Sintering in nitrogen atmosphere produced much more complicated shrinkage behavior. Thus, all the compositions exhibit multiple steps of shrinkage varying from two in case of AlN-Y_2O_3 sintering additives to up to five in the case of AlN-La_2O_3 ones. Moreover, in this case the increase of α-SiC content in the initial mixtures have a rather pronounced effect on the densification behavior reducing the number of the shrinkage rate maximums (see Figs. 4 (a) and (b)). Also the nitrogen sintering atmosphere obviously hinders the densification of Y_2O_3 containing compositions while substantially enhancing the densification of the La_2O_3 containing ones as compared to the argon sintering atmosphere.

What should be specifically emphasized is that the presence of multiple peaks on the shrinkage rate *vs.* temperature curves, which are most pronounced in Fig. 4 (a), indicate a rather complicated sequence of phase formation on heating. Actually, each minimum on the curve indicates a crystalline phase formation, which hinders densification. And only with the further increase of temperature, when the melting point of the formed phase is reached densification proceeds further. All these observations lead to a conclusion that the phase relationships in the AlN-RE_2O_3 systems with the RE element other than Y are different from the ones in the AlN-Y_2O_3 system. Therefore, in order to optimize the sintering procedure for AlN-RE_2O_3 additive systems further investigation of phase relations for these materials is necessary. The next step that is planned is to follow up the exact sequence of phase formation on heating in the systems of choice with the aim of thermal sintering schedule optimization.

In the case of Y_2O_3 doped materials, the first of the observed peaks on the shrinkage rate *vs.* temperature curve while sintering in nitrogen is tentatively attributed to initial and limited liquid phase formation with the participation of surface oxides SiO_2 and Al_2O_3 present on SiC and AlN powders particles, respectively, and Y_2O_3. The phase pre-

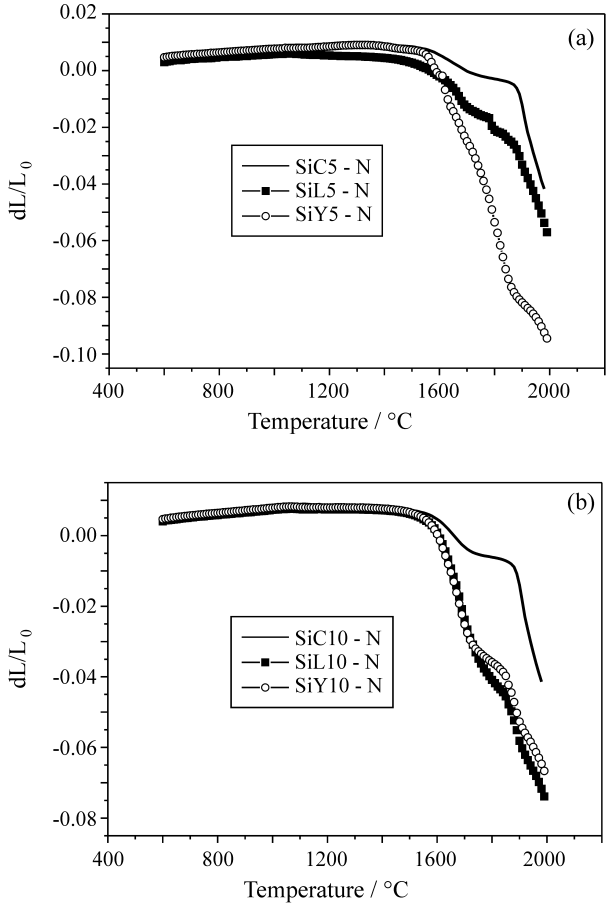

Figure 3. The results of dilatometric experiments: linear shrinkage *vs.* temperature while sintered in nitrogen: a) 5wt% α-SiC; b) 10wt% α-SiC.

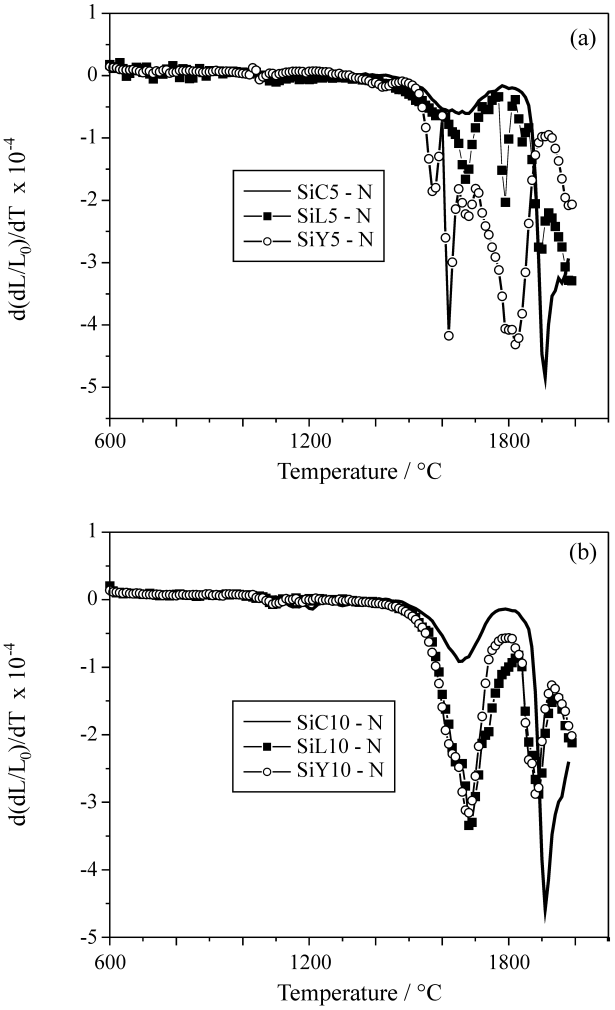

Figure 4. The results of dilatometric experiments: shrinkage rate *vs.* temperature while sintered in nitrogen: a) 5wt% α-SiC; b) 10wt% α-SiC.

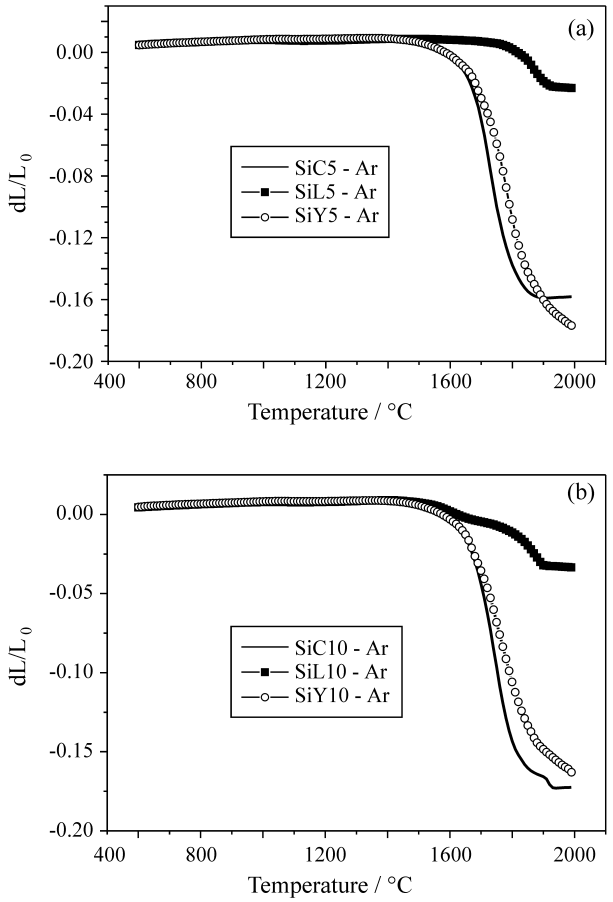

Figure 5. The results of dilatometric experiments: linear shrinkage *vs.* temperature while sintered in argon: a) 5wt% α-SiC; b) 10wt% α-SiC.

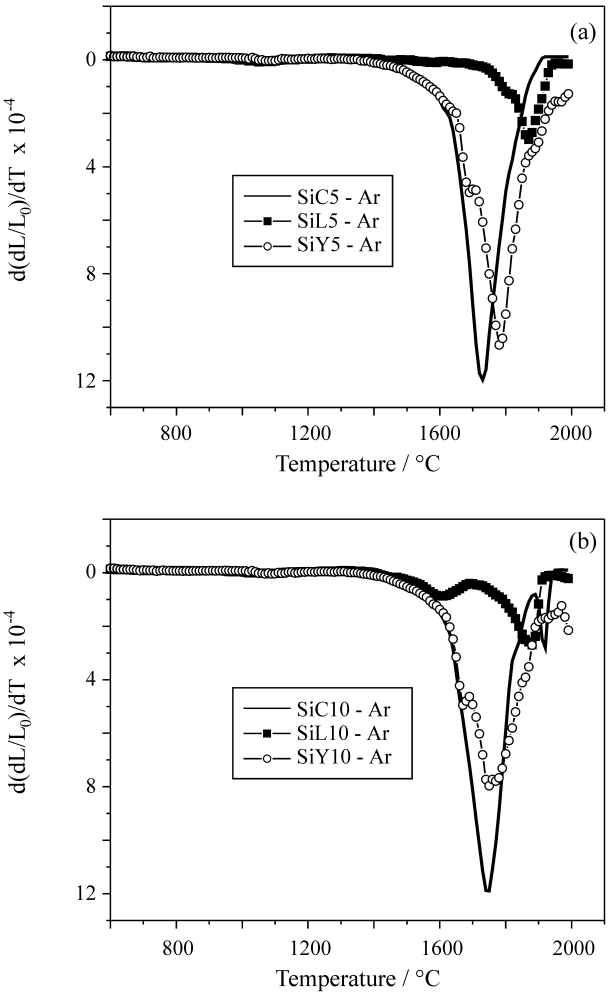

Figure 6. The results of dilatometric experiments: shrinkage rate *vs.* temperature while sintered in argon: a) 5wt% α-SiC; b) 10wt% α-SiC.

cipitating at about 1700 °C and subsequently melting at about 1800 °C was not identified until now.

Based on the results of the dilatometric investigations the time-temperature sintering schedule for furnace sintering was developed as presented in Fig. 7. The results of the furnace sintering of the prepared compositions in nitrogen and argon are presented in Table 2.

As it can be seen, the developed sintering schedule while being almost optimal for Y_2O_3 containing compositions needs further refinement for the other compositions of choice in order to achieve higher sintered densities. Overall, the furnace sintering results are consistent with dilatometric measurements, although the conditions of sintering in both cases are not identical at least in regard of the stagnant atmosphere in the former case, which practically means very different partial pressures of the volatile components forming during sintering. As it was mentioned in the introduction to the present paper, the sintering atmosphere in the sense of the partial pressures of the volatile products is a very important factor in densification, and apparently also needs further scrutiny.

Among the most obvious results of the furnace sintering it should be noted that the Yb_2O_3 containing compositions exhibit the highest weight loss both in argon and in nitrogen, while the La_2O_3 containing ones have the lowest weight loss in both cases. Also the so far best results as to the sintered densities were achieved with the Y_2O_3 containing compositions while sintered in argon.

In order to establish the possibility of in-situ platelet reinforcement of the liquid phase sintered SiC ceramics, post sintering heat treatment in N_2 atmosphere at 1900 and 1950 °C was carried out. Such a treatment had a goal of promoting of the β-SiC to α-SiC phase transformation, which occurred only to a minor extent during sintering. The kinetics of the above mentioned phase transformation was studied by means of XRD in relation to the composition of the sintering additives used.

Severe overlapping of the reflexes of β-SiC due to the polytypism of SiC makes the quantitative phase analysis extremely difficult. However, the existing three well de-

Table 2. Green density, sintered density and weight loss after furnace sintering of investigated compositions.

Composition	Atmosphere of sintering	Green density % td	Apparent density g/cm^3	Relative density % td	Weight loss %
SiC5	nitrogen	55.1	2.90	86.8	2.70
	argon	55.2	3.25	97.3	3.21
SiC10	nitrogen	55.1	2.86	85.6	2.54
	argon	55.1	3.24	97.0	2.99
SiL5	nitrogen	55.2	3.29	94.6	0.94
	argon	55.1	2.71	77.9	2.13
SiL10	nitrogen	55.1	3.28	94.3	1.39
	argon	55.2	2.62	75.3	2.48
SiY5	nitrogen	55.1	3.41	92.4	5.13
	argon	55.2	3.42	92.6	6.09
SiY10	nitrogen	55.1	3.40	92.1	4.25
	argon	55.2	3.39	91.7	5.28

fined α-SiC reflexes (6H-polytype) (see Fig. 8) enable to quantitatively evaluate the extent of the phase transformation by normalizing the sum of the $(111)_{3C}$ and $(006)_{6H}$ reflexes intensities. Using this approach, a calibration curve can be obtained by applying the inner standard technique, *i.e.*, a series of powder mixtures of β-SiC with fixed α-SiC additions was analyzed by XRD, and the ratio between the relevant reflexes intensities was determined. Thus obtained curve, presented in Fig. 9, was subsequently used for the extent of phase transformation during post sintering heat treatment determination.

The results of post sintering heat treatment and of the β-SiC to α-SiC phase transformation kinetics are presented in Fig. 10. As it can be seen, the β-SiC to α-SiC phase transformation occurs more readily with the La_2O_3 additions, while Y_2O_3 containing materials exhibit a somewhat sluggish behavior. At present time, only a tentative explanation is possible attributing such behavior to better condi-

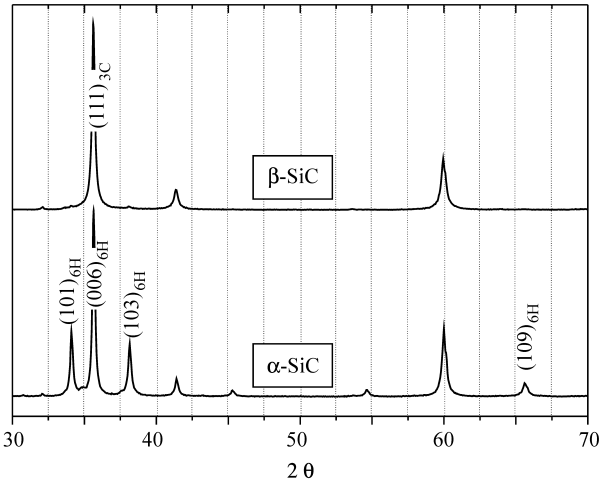

Figure 8. X-ray diffractograms of α-SiC and β-SiC powders (standards).

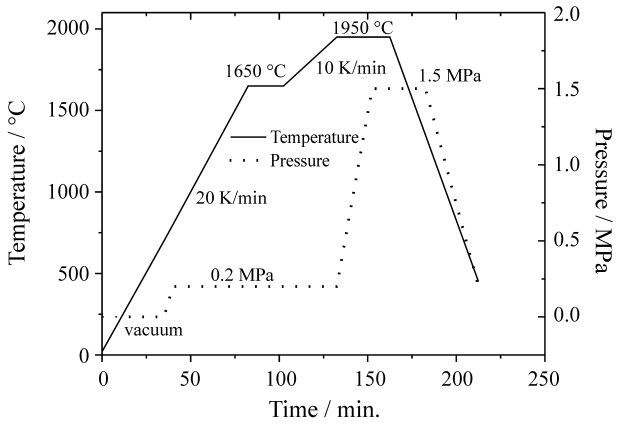

Figure 7. The time-temperature- gas pressure schedule of the furnace sintering of the materials.

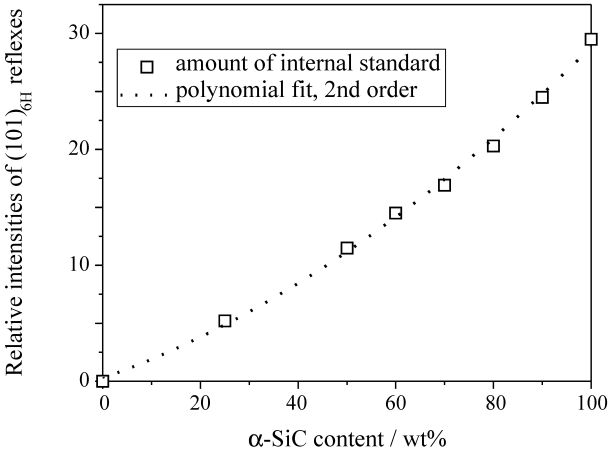

Figure 9. Calibration curve for α-SiC quantitative determination obtained by inner standard techniques.

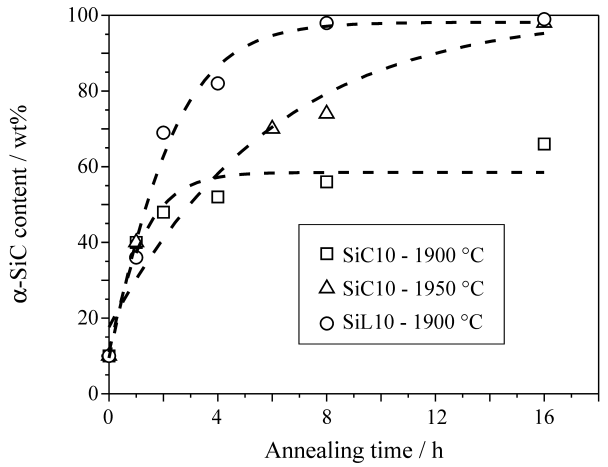

Figure 10. Results of β-SiC to α-SiC phase transformation kinetics investigation.

tions for diffusion provided by the secondary phases formed in La_2O_3 doped materials. However, further more detailed investigation of the processes involved is necessary.

The microstructure of the as-sintered and thermally treated SiC-AlN-Y_2O_3 material are presented on Fig. 11. While the as-sintered sample has a fine uniaxial grain morphology, the annealed material exhibits microstructure with elongated grain morphology as a result of the β-SiC to α-SiC transformation. The grain growth occurred as well, thus providing evidence of transformation controlled grain growth mechanism.

4. Conclusions

Silicon carbide can be sintered up to high densities by means of liquid phase sintering under low gas pressure with AlN-Y_2O_3, AlN-Yb_2O_3, and AlN-La_2O_3 sintering additives. As-sintered materials exhibited fine-grained homogeneous microstructure.

Densification behavior of materials with Y_2O_3 and La_2O_3 additions is shown to be inverse: While the former materials densify better in Ar, the latter show better sinterability in N_2. Moreover, the densification of La_2O_3 containing materials has a complex nature most probably due to a complex phase formation sequence on heating. This phenomenon needs further investigation. The Yb_2O_3 containing materials exhibited sintering behavior more similar to the behavior of Y_2O_3 containing ones.

Transformation controlled grain growth during post sintering heat treatment of the developed materials was established. A high degree or even a complete β-SiC to α-SiC transformation was achieved by such techniques in reasonably short time intervals. The kinetics of the phase transformation was shown to depend on the composition of sintering additives, the use of less refractory RE oxides

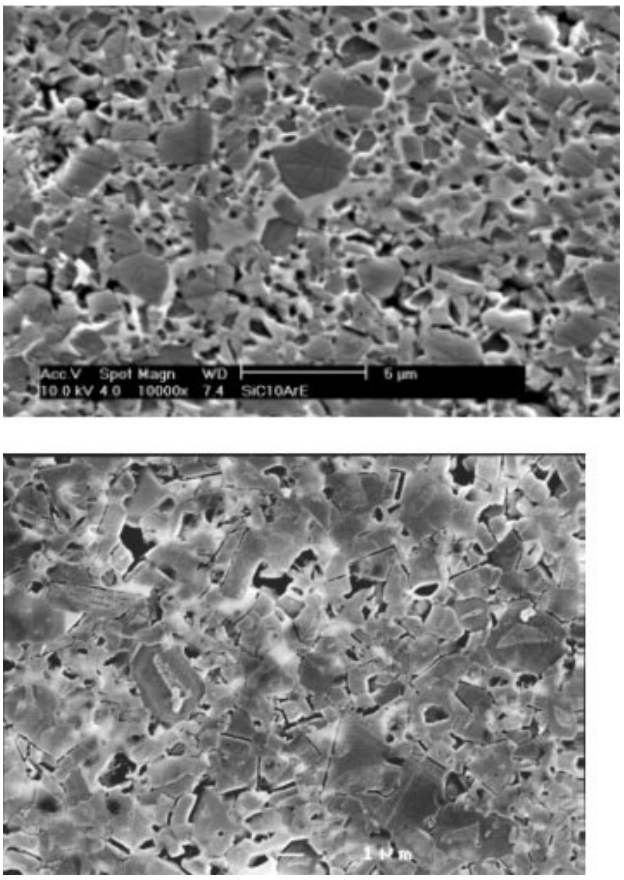

Figure 11. Microstructures of the (a) as-sintered (1 h at 1950 °C in Ar atmosphere) and (b) annealed (8 h at 1900 °C, N_2 atmosphere) SiC-AlN-Y_2O_3 chemically etched samples.

accelerating the process. Thus, the possibility of in-situ platelet reinforced SiC ceramics was shown.

Further research aimed at the optimization of both composition and processing of the materials under development is necessary.

Acknowledgements

The authors would like to express their gratitude to CNPq for financial support of Dr. V. Izhevskyi's participation in this research.

Present research is supported by PRONEX/FINEP, and by FAPESP projects 97/01114-5 and 96-9604/9.

The authors would also like to thank CPP/IPEN (Centro de Processamento de Pós) for the use of sintering facilities.

References

1. Prochaska, S. The role of boron and carbon in sintering of silicon carbide. *Special Ceramics 6*, Popper, P., ed. The British Ceramic Research Association, Stoke-on-Trent, U.K., p. 171-81, 1975.
2. Cutler, R.A.; Jackson, T.B. Liquid phase sintered silicon carbide. *Ceramic Materials and Components for Engines*, Proceedings of the Third International Sym-

posium. Tennery, V.J., ed. American Ceramic Society, Westerwille, OH, p. 309-18, 1989.

3. Mulla, M.A.; Krstic, V.D. Low-temperature pressureless sintering of β-silicon carbide with aluminum oxide and yttrium oxide additions. *Am. Ceram. Soc. Bull.*, v. 70, n. 3, p. 439-443, 1991.
4. Mulla, M.A.; Krstic, V.D. Pressureless sintering of β-SiC with Al_2O_3 additions. *J. Mater. Sci.*, n. 29, p. 934-938, 1994.
5. Lee, S.K.; Kim, C.H. Effects of α-SiC *vs.* β-SiC starting powders on microstructure and fracture toughness of SiC sintered with Al_2O_3-Y_2O_3 additives. *J. Am. Ceram. Soc.*, v. 77, n. 6, p. 1655-1658, 1994.
6. Omori, M.; Takei, H. Pressureless Sintering of SiC. *J. Am. Ceram. Soc.*, v. 65, n. 6, p. C-92, 1982.
7. Padture, P. *In-situ* toughened silicon carbide. *J. Am. Ceram. Soc.*, v. 77, n. 2, p. 519-523, 1994.
8. Kim, W.J.; Kim, Y.-W. Liquid-phase sintering of silicon carbide. *J. Kor. Ceram. Soc.*, v. 32, n. 10, p. 1162-1168, 1995.
9. Bocker, W.; Landfermann, H.; Hausner, H. Sintering of α-silicon carbide with additions of aluminium. *Powd. Metall. Intern.*, v. 11, p. 83-85, 1979.
10. Negita, K. Effective sintering aids for silicon carbide ceramics: reactivities of silicon carbide with various additives. *J. Am. Ceram. Soc.*, v. 69, n. 12, p. C-308-C310, 1986.
11. Chia, K.Y.; Boecker, W.D.G.; Storm, R.S. Silicon carbide bodies having high toughness and fracture resistance and method of making same. United States Patent, 5.298.470, USA, 1994.
12. Keppeler, M.; Reihert, H.-G.; Broadly, J.M.; Turn, G.; Wiedmann, I.; Aldinger, F. High temperature mechanical behavior of liquid phase sintered silicon carbide. *J. Eur. Ceram. Soc.*, v. 18 p. 521-26, 1998.
13. Ruh, R.; Zandvil, A. Compositions and properties of hot-pressed SiC-AlN solid solutions. *J. Am. Ceram. Soc.*, v. 65, n. 5, p. 260-265, 1982.
14. Zangvil, A.; Ruh, R. The $Si_3Al_4N_4C_3$ and $Si_3Al_5N_5C_3$ compounds as SiC-AlN solid solutions. *J. Mat. Sci. Lett.*, v. 3, p. 249-250, 1984.
15. Zangvil, A.; Ruh, R. Solid solutions and compositions in the SiC-AlN and SiC-BN systems. *Mat. Sci. Eng.*, v. 71, p. 159-164, 1985.
16. Zangvil, A.; Ruh, R. Phase relationships in the silicon carbide-aluminum nitride system. *J. Am. Ceram. Soc.*, v.71, n. 10, p. 884-890, 1988.
17. Lee, J.-K.; Tanaka, H.; Otami, S. Preparation of SiC-AlN composites by liquid-phase sintering and their microstructure. *J. Ceram. Soc. Japan*, v. 103, n. 9, p. 873-877, 1995.
18. Singhal, L.S.; Kleebe, H.-J. Core/rim structure of liquid-phase-sinterd silicon carbide. *J. Am. Ceram. Soc.*, v. 76 p. 773-776, 1993.
19. Lee, L.S.K.; Kim, Y.C.; Kim, C.H. Microstructural development and mechanical properties of pressureless-sintered SiC with plate-like grains using Al_2O_3-Y_2O_3 additions. *J. Mater. Sci.*, v. 29, p. 5321-526, 1994.
20. Jeutter, A. Untersuchung der Phasenbezieung im Sysytem Aluminiumnitrid-Yttriumoxid. Diplomarbeit an Universitat Stuttgart, 1993.

The publication costs of this article were covered by FAPESP